Effect of Drawing on Creep Fracture of Polypropylene Fibers

AKIRA TAKAKU, *Department of Textile and Polymeric Materials, Tokyo Institute of Technology, O-okayama, Meguro-ku, Tokyo, Japan*

Synopsis

The ultimate properties of polypropylene fibers, prepared by drawing the same undrawn fibers to different draw ratios, were determined by the creep fracture method at temperatures from 40 to 120°C. The composite curves of the engineering stress at break, the true stress at break, and the ultimate extension ratio were constructed as a function of reduced time to break by assuming time–temperature superposition. The temperature dependence of the shift factor a_T used in the superposition could be represented by a single equation of the Williams, Landel, and Ferry form. The composite curves of the true stress at break for the samples with different draw ratios were almost the same independently of draw ratio. The composite curves of the ultimate extension ratio for these samples could be reduced to a single curve by assuming that the ultimate extension ratio evaluated with respect to the unit length of the undrawn fibers were constant independently of draw ratio if the time to break and temperature conditions of the measurement were fixed constant. A possible fracture mechanism is discussed on the basis of the fracture mechanisms proposed by Samuels and Peterlin.

INTRODUCTION

Hall[1] has found that the ultimate properties of drawn isotactic polypropylene fibers, which have a glass transition temperature below room temperature, are sensitive to changes in temperature and experimental time scale. The ultimate properties of the polypropylene fibers seem closely allied to viscoelastic properties of the fibers. For elastomers, Smith[2,3] has found that the time–temperature superposition applied to their linear viscoelastic properties is also applicable to the ultimate properties. A number of works have been reported on the application of the time–temperature superposition to the viscoelastic properties of crystalline polymers. Fujino et al.[4] and Mercier et al.[5] have found for poly(vinyl acetates) and partially crystallized polycarbonate, respectively, that the time–temperature superposition of the Williams, Landel and Ferry (WLF) form is valid.[6] Takemura[7] and Nagamatsu[8] have shown for the stress relaxation of polyethylene that the combination of a vertical shift along the logarithmic axis of relaxation modulus with a horizontal shift along the logarithmic axis of time gives a composite curve. The stress–strain relation of crystalline polymers is apparently nonlinear in general. Hence, the applicability of these time–temperature superposition techniques may be limited to the viscoelastic properties in small deformations.

It was reported in the previous article[9] that, apart from the problem of the deformation up to fracture, the smooth composite curve of the tensile strength and of the ultimate strain for polypropylene fibers could be obtained by assuming a time–temperature superposition in the relationship of time to break versus temperature determined by creep fracture experiments. The temperature de-

Journal of Applied Polymer Science, Vol. 26, 3565–3573 (1981)
 CCC 0021-8995/81/113565-09$01.00

pendence of the shift factor adopted for the superposition followed an equation of the WLF form. A more direct test should be required to ensure the applicability of the superposition to the ultimate properties of polypropylene fibers. However, applying the superposition to polypropylene fibers with different characteristics and seeing what results will be also helpful to evaluate the validity of the superposition.

In the present study, time–temperature superposition has been applied to the ultimate properties of polypropylene fibers prepared by drawing the same undrawn fibers to different draw ratios. An attempt has been made to detect what systematic changes appear in the time–temperature dependence of the ultimate properties of those fibers, and a possible fracture mechanism is discussed.

MATERIALS

Isotactic polypropylene fibers in the form of continuous filament yarn spun by conventional melt spinning were used as a starting material. The as-spun filament yarn was drawn at three different draw ratios on a roller drawing apparatus at 130°C. The drawn filament yarns were heat-treated at 130°C for 30 min in the fixed state on a frame before measurements. The characteristics of these heat-treated fibers are shown in Table I. The draw ratio was calculated as the ratio of the linear density of fibers before drawing against that of the fibers after drawing. The intrinsic viscosity was determined at 135°C in tetraline. The birefringence was measured on a polarizing microscope with a Berek compensator. The density was measured in an isopropyl alcohol–water density gradient column at 30°C.

EXPERIMENTAL

The ultimate properties of the polypropylene fibers were determined by a creep fracture method. The creep fracture experiments were carried out by putting a static tensile load on the lower end of a yarn specimen hung in an oven. The time to break, which was the time required after the application of a load to a specimen until the specimen broke, and the elongation at break were measured. The original specimen length used was 5 cm. The temperature in the oven was controlled at the desired temperatures with a precision of ±0.5°C.

The expressions engineering stress at break, true stress at break, and ultimate extension ratio are employed in this article. The engineering stress at break σ_b is given by the load per unit area of the original cross section of a specimen before the application of the load. The true stress at break is defined as the load per unit area of the instantaneous cross-sectional area of a specimen when it breaks. The true stress at break was calculated as $\lambda_b \sigma_b$, where λ_b is the ultimate exten-

TABLE I
The Characteristics of Polypropylene Fibers Used in Creep Fracture Experiments

Sample	Draw ratio	Linear density, tex/fils.	Intrinsic viscosity, dL/g	Birefringence $\times 10^3$	Density, g/cm^3
PP83	2.7	8.16/15	1.01	30.6	0.9057
PP84	3.5	6.38/15	1.01	32.0	0.9047
PP85	4.5	4.94/15	1.01	33.2	0.9044

sion ratio. This ultimate extension ratio is defined as the ratio of the specimen length at break against the initial length before the application of a load. The natural logarithm of λ_b corresponds to the true strain at break.

The original cross-sectional area was calculated from the linear density and density of the fibers.

RESULTS AND DISCUSSION

Composite Curves of Engineering Stress at Break

It has been shown for polypropylene fibers[9] that the composite curve of the tensile strength (engineering stress at break) versus the time to break t_b can be obtained by applying time–temperature superposition. The time–temperature superposition applied is written as

$$t_{b,T} = a_T t_{b,T_0} \tag{1}$$

where a_T is a shift factor, and T and T_0 denote experimental and reference temperatures, respectively. The temperature dependence of the shift factor a_T adopted for the superposition is represented by the equation of the WLF form, as follows:

$$\log a_T = -\frac{13.64(T - T_0)}{146.8 + T - T_0} \tag{2}$$

where T_0 is selected at 313 K.

Figure 1 shows the composite curve of the engineering stress at break against time to break for samples PP83, PP84, and PP85, constructed by applying the time–temperature superposition of eq. (1). In Figure 1, the reference temperature chosen is 40°C. The values of the shift factor a_T used in the superposition are shown in Figure 2, where the ordinate values are shifted arbitrary amounts A for clarity.

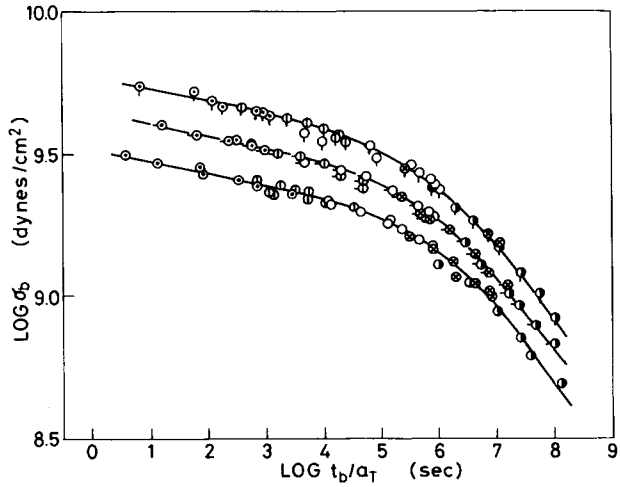

Fig. 1. Composite curves of engineering stress at break σ_b vs. reduced time to break t_b/a_T for polypropylene fibers prepared at different draw ratios, where reference temperature is 40°C. Samples: (○) PP83; (–○) PP84; (♀) PP85. Temperature (°C): (⊙) 40; (⊕) 60; (○) 80; (⊗) 100; (◑) 120.

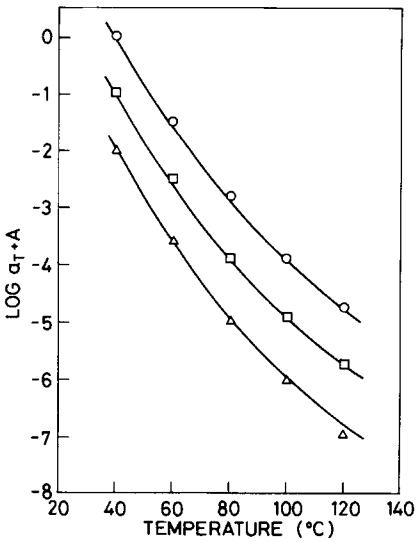

Fig. 2. Relation of shift factor a_T with temperature. Values of A are arbitrary. Points represent experimental values. Samples: (○) PP83, $A = 0$; (□) PP84, $A = -1.0$; (△) PP85, $A = -2.0$. Solid lines calculated from eq. (1).

The continuous curves in Figure 2 indicate the calculated curve from eq. (2). Equation (2) well represents the relation of the experimental values of a_T with temperature for samples PP83, PP84, and PP85.

Figure 1 shows that the higher the draw ratio is, the higher the engineering stress at break if time to break is constant. This feature does not change with a choice of reference temperature, since the temperature dependence of the shift factor a_T is approximately the same for all polypropylene fibers used.

Composite Curves of True Stress at Break and Ultimate Extension Ratio

Figure 3 shows the composite curves of the true stress at break $\lambda_b \sigma_b$ against time to break for samples PP83, PP84, and PP85, where the reference temperature chosen is 40°C. In this figure, the ordinate values are shifted arbitrary amounts B for clarity. The composite curves of true stress at break of the samples with different draw ratios were constructed by using the same values of a_T adopted to construct the composite curves of engineering stress at break for the respective samples.

Figure 4 shows the composite curves of the ultimate extension ratio λ_b versus time to break at a reference temperature of 40°C. These composite curves were also constructed by using the same values of a_T adopted to construct the composite curve of engineering stress at break for the respective samples.

Variation of Creep Fracture Properties with Drawing

The composite curves of true stress at break in Figure 3 are reproduced in Figure 5 without the arbitrary amounts B introduced in Figure 3. It is noted in Figure 5 that the composite curves of true stress at break for the various

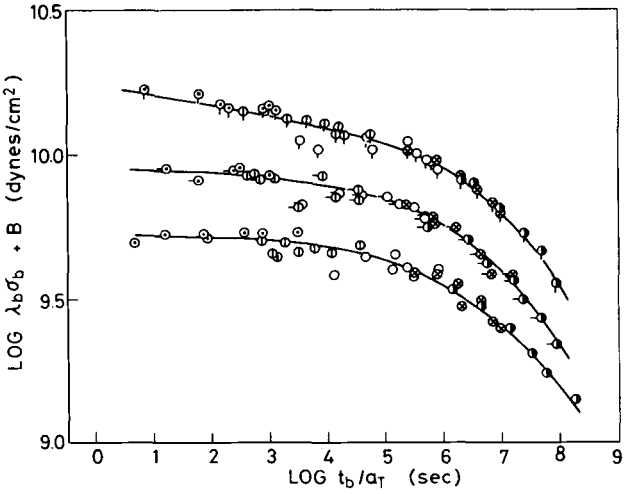

Fig. 3. Composite curves of true stress at break $\lambda_b\sigma_b$ vs. reduced time to break t_b/a_T for polypropylene fibers prepared at different draw ratios, where reference temperature is 40°C. Values of B are arbitrary. Samples: (O) PP83, $B = 0$; (—O) PP84, $B = 0.2$; (Q) PP85, $B = 0.4$. Temperature references are the same as in Fig. 1.

samples are almost the same over the entire time scale obtained. That is, denoting the arbitrary and reference samples possessing different draw ratios by the suffixes i and r, respectively, we may write the relation

$$\lambda_{b,i}(t_b)\,\sigma_{b,i}(t_b) = \lambda_{b,r}(t_b)\,\sigma_{b,r}(t_b) \tag{3}$$

Assume that the ultimate extension ratio calculated against the unit length of the undrawn fibers is constant independently of draw ratio if the time to break and temperature conditions are fixed constant. Since the samples used in this study were prepared from the same undrawn fibers, by denoting D_R as draw ratio and by defining α as the ratio of $D_{R,r}$ against $D_{R,i}$, the following relation may be written:

$$\alpha = \frac{D_{R,r}}{D_{R,i}} = \frac{\lambda_{b,i}(t_b)}{\lambda_{b,r}(t_b)} = \frac{\sigma_{b,r}(t_b)}{\sigma_{b,i}(t_b)} \tag{4}$$

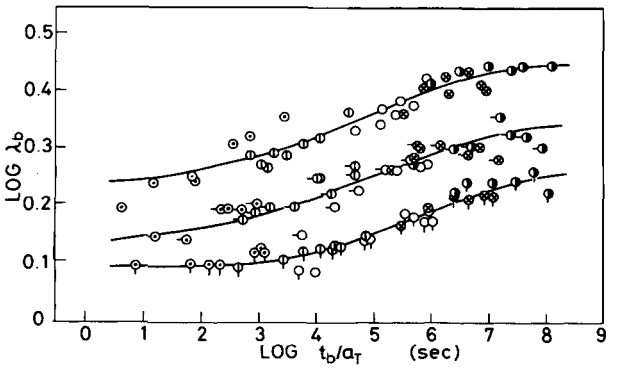

Fig. 4. Composite curves of ultimate extension ratio λ_b vs. reduced time to break t_b/a_T for polypropylene fibers prepared at different draw ratios, where reference temperature is 40°C. Samples: (O) PP83; (—O) PP84; (Q) PP85. Temperature references are the same as in Fig. 1.

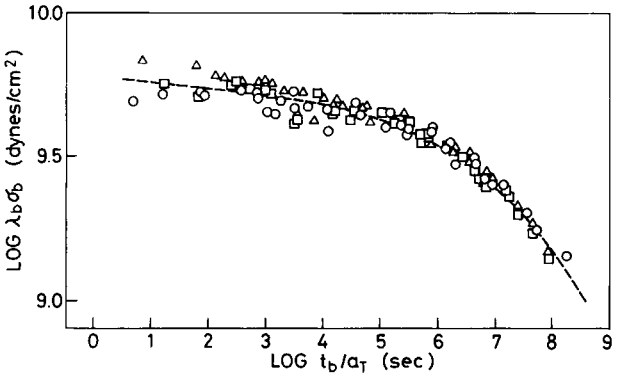

Fig. 5. Reproduction of the composite curves of true stress at break in Fig. 3. Samples: (○) PP83; (□) PP84; (△) PP85.

That is, the plot of λ_b/α or $\alpha\sigma_b$ against t_b/a_T for an arbitrary sample would be consistent with the plot of λ_b or σ_b against t_b/a_T for a reference sample, respectively. Figure 6 shows the plots of log λ_b/α against log t_b/a_T for the samples with different draw ratios, where the reference temperature is 40°C and the reference sample is sample PP83. The values of α were calculated by using the values of the draw ratio shown in Table I. In Figure 6, the plots for the different samples well overlap one another, although the scatter of the data is fairly large. Figure 7 shows the plots of log $\alpha\sigma_b$ versus log t_b/a_T, where the reference temperature and the reference sample are the same as those in Figure 6, respectively. The results in Figures 6 and 7 indicate that the simple assumption given by eq. (4) works well.

Samuels[10] has considered that when polypropylene fibers possessing various initial orientations are deformed under the proper conditions, they can reach a definite final structure yielding a definite true stress at break. According to Samuels, in any sample of a polymer there is a distribution of flaws which can cause crack formation and ultimate fracture. Opposed to the failure mechanism is the ability of the sample to deform plastically to relieve and redistribute the stress. If a sample is deformed slowly enough, the molecules have enough mobility and time to rearrange the internal structure. The spherulitic structure slowly destroyed, a microfibrillar structure develops, stress builds up in the microfibrillar structure, and finally the flaw mechanism predominates as no

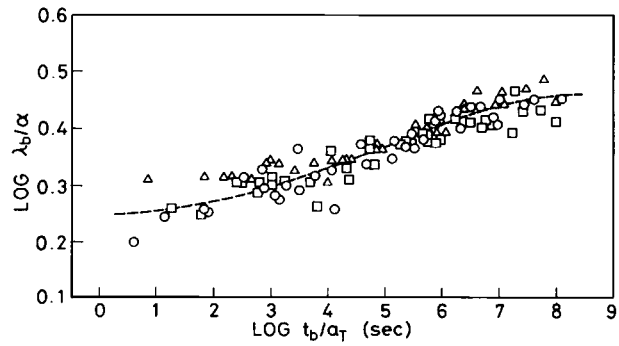

Fig. 6. Plots of log λ_b/a against log t_b/a_T. Samples: (○) PP83; (□) PP84; (△) PP85.

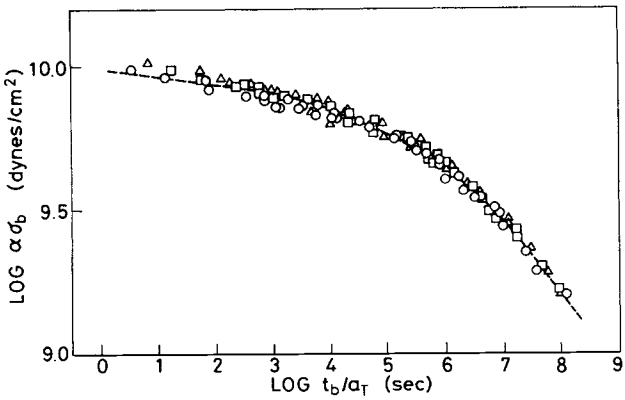

Fig. 7. Plots of log $a\sigma_b$ vs. log t_b/a_T. Samples: (○) PP83; (□) PP84; (△) PP85.

further plastic deformation mechanisms are available and the sample fractures. The final structure at break will be the microfibrillar structure thermodynamically stable at the deformation temperature at the moment the failure mechanism takes control, and that final structure will be independent of the initial orientation state of the sample. The samples with various initial orientations can all reach the same microfibrillar structure, and they will each have a definite extension to which they must deform, and that extension is determined by their initial orientation state. As in the case of the present experiments, if the drawn samples are the ones prepared from the same undrawn sample and the ultimate extensions of those drawn samples are determined with respect to the unit length of the starting undrawn sample, the ultimate extensions will take a definite value independently of the orientation state of the drawn samples.

The creep fracture experiments in the present study were carried out on relatively longer time scales at temperatures above the glass transition temperature. The experimental conditions adopted would be enough to allow the rearrangement of the internal structure of the samples in the deformation process up to fracture. Therefore, the consideration of Samuels could be applied to explain the rules depicted in Figures 5, 6, and 7. In other words, the polypropylene fibers seem to show a fracture behavior corresponding to the consideration of Samuels over the longer time scales and wide temperature range of measurement if the fibers fracture under the proper conditions.

As is shown in Figure 5, the samples with different draw ratios represent the same relation of the true stress at break with the time to break. This suggests that the samples are predominated at the extreme by a definite fracture mechanism peculiar possibly to the microfibrillar structure. The fracture mechanism seems dependent strongly on the viscoelastic properties expected of amorphous molecules. To this point, a fracture mechanism proposed by Peterlin[11] on the basis of a microfibrillar model of oriented crystalline polymers will be pertinent.

In the model of Peterlin, the microfibrils consist of folded-chain crystal blocks alternating with amorphous layers bridged by a great many tie molecules. A bundle of the microfibrils forms a fibril, and in the fibril an additional thin pseudo-amorphous boundary layer exists between the adjacent microfibrils. The material connection by tie molecules in the direction of the fiber axis is almost

completely interrupted at each microfibrillar end. A longitudinal stress cannot be transmitted through such a microfibrillar end because of the lack of the material connection by tie molecules. Therefore, under axial stress a slip between the microfibril with free end and the adjacent microfibrils occurs near the microfibrillar end, and this can cause the stress concentration to the adjacent microfibrils. Peterlin called the microfibrillar end a point vacancy defect of a microfibrillar lattice of the fibrous structure. With increasing load, the elastic energy accumulation at point vacancies becomes sufficient for microcrack formation. The elastic energy U required for the microcrack formation is estimated to be of the order

$$U = A_{mf} L_{pv} \sigma^2 / 2E_a \tag{5}$$

where A_{mf} is the cross-sectional area of the microfibril, L_{pv} is the length of a point vacancy along the microfibrillar axis, σ is the stress on a point vacancy in the direction of the microfibrillar axis, and E_a is the modulus of the amorphous region. It is noted that the contribution of the crystals to the elastic energy U can be neglected since the elastic modulus of the crystals is so much larger than that of the amorphous regions.

The fracture mechanism of Peterlin, as summarized by eq. (5), indicates that the formation of the microcrack at the microfibrillar end depends on the viscoelastic nature of the amorphous regions near the microfibrillar end. The forces opposed to the deformation at a point vacancy are the van der Waals forces on the amorphous regions. It is possible, therefore, that the time–temperature superposition applicable to amorphous polymers could be effected on the elastic energy required for the microcrack formation at a point vacancy. The propagation of a crack after the microcrack has reached a critical size would be more or less catastrophic; hence, the time–temperature dependence of the microcrack formation will determine the macroscopic fracture behavior of polypropylene fibers.

It can be stated conclusively that the true stress at break of polypropylene fibers prepared at various draw ratios is approximately constant if time to break and temperature are constant. This indicates that a creep fracture criterion of polypropylene fibers could be represented by a specified true stress given, independently of draw ratio, as a function of time to break and temperature. For elastomers,[12,13] it is known that the functional relation between tensile strength and ultimate strain is independent of time scale. It will be apparent that for polypropylene fibers, a functional relation between tensile strength and ultimate extension ratio is independent of time scale and temperature within the limit of the present creep fracture experiments, because the tensile strength and the ultimate extension ratio of the fibers at different temperatures could be reduced to those at a reference temperature by using the same temperature dependent factor a_T. Furthermore, in case of the polypropylene fibers prepared from the same undrawn fibers, a constant functional relation independent of draw ratio seems to exist between the true stress at break and the ultimate extension ratio evaluated with respect to the unit length of the undrawn fibers.

This work was carried out by the author at the Central Research Laboratory of Mitsubishi Rayon Co., Ltd.

References

1. I. H. Hall, *J. Polym. Sci.*, **54,** 505 (1961).
2. T. L. Smith, *J. Polym. Sci.*, **32,** 99 (1958).
3. T. L. Smith, *Trans. Soc. Rheol.*, **6,** 61 (1962).
4. J. P. Mercier and G. Groeninckx, *Rheol. Acta*, **8,** 510 (1969).
5. K. Fujino, K. Senshu, T. Horino, and H. Kawai, *J. Colloid Sci.*, **18,** 119 (1963).
6. M. L. Williams, R. F. Landel, and J. D. Ferry, *J. Am. Chem. Soc.*, **77,** 3707 (1955).
7. T. Takemura, *J. Polym. Sci.*, **38,** 471 (1959).
8. K. Nagamatsu, *Kolloid-Z. Z. Polym.*, **172,** 141 (1962).
9. A. Takaku, *J. Appl. Polym. Sci.*, **25,** 1861 (1980).
10. R. J. Samuels, *J. Macromol. Sci.*, **B4,** 701 (1970).
11. A. Peterlin, *J. Macromol Sci.*, **B8,** 83 (1973).
12. T. L. Smith and P. J. Stedry, *J. Appl. Phys.*, **31,** 1892 (1960).
13. T. L. Smith, *J. Polym. Sci., Part A*, **1,** 3957 (1963).

Received August 29, 1980
Accepted May 5, 1981